

ANALYSIS OF THE PROCESS OF MIXING OF A PASSIVE IMPURITY IN A JET MIXER

V. L. Zhdanov,^a A. D. Chorney,^b
and E. Hassel^a

UDC 532.517.4,532.526.5

The experimental results for two regimes of mixing of a passive impurity in an axisymmetric jet mixer — the mixing of a turbulent jet and a cocurrent flow to form a recirculation zone behind the nozzle and an analogous mixing without the formation of a recirculation zone ($Re_d = 10,000$) — have been presented. The velocity field has been measured in the mixer cross sections at different distances from the nozzle ($0.1 < x/D < 9.1$) with a one-component Doppler laser anemometer, whereas the scalar field (concentration of the passive impurity) has been diagnosed by the laser-induced fluorescence method. Based on the scalar distributions obtained, the autocorrelation function and the integral scale have been computed, the form of the probability density function has been restored, and the distributions of the asymmetry and excess coefficients have been constructed. Visualization of flow in the mixer has been carried out.

Introduction. Axisymmetric jet mixers currently used in the chemical and food industries are quite simple technical devices; they represent two pipes of different diameter installed coaxially. Despite their simplicity, they make it possible to implement both the laminar and turbulent mixing of media and to combine these processes by selecting the ratio of the flow rates of the initial media. In this work, we consider the mixing of a turbulent jet blown out of the nozzle with a cocurrent flow where the transient hydrodynamic regime of flow is implemented. The jet velocity exceeds the cocurrent-flow velocity. Possible mixing regimes are reduced to two fundamentally different types: (1) a recirculation zone of flow is formed immediately behind the nozzle and (2) no recirculation zone behind the nozzle is formed. Conditions for generation of these mixing regimes are determined from the flow-rate-to-diameter ratio [1]: (1) $D/d > 1 + Q_D/Q_d$ is the mixing with a recirculation zone and (2) $D/d < 1 + Q_D/Q_d$ is the mixing without a recirculation zone. The average-velocity field in the first regime has been described in detail in [2], where it has been established that the leading edge and center of the recirculation zone shift from the nozzle as the flow-rate ratio grows, but the boundary of its degeneration is constant and is located at a distance $x/D \sim 3$. Clearly, the complex structure of the flow with a high level of pulsations ($\sim 40\%$) in the recirculation region will contribute to a faster equalization of the concentration of the passive impurity over the mixer cross section. In [2], the average velocity was measured with a Pitot tube, whereas the pulsation velocities were recorded by the hot-wire-anemometer sensor only on the mixer axis: taking account of the high level of turbulence, this allowed just a qualitative analysis of their behavior. It was noted [2] on the photographs with an exposure time of 1/20 sec that the jet is deflected from its axis of symmetry in interaction with the recirculation zone where there are numerous vortices whose size and position substantially vary with time. However, in the work mentioned, the recirculation zone is considered as a 3D stationary symmetric vortex formed around the jet, i.e., the nonstationary phenomena observed are disregarded.

The regime of mixing without a recirculation zone is used, e.g., in chemical reactors where we have competitive reactions. In this case, it is necessary to rapidly remove the end product from the reaction zone to avoid the interaction of this product with the starting components.

^aFachbereich Maschinenbau und Schiffstechnik, Lerhsthul für Technische Thermodynamik, Uviversität Rostok, 2 A. Einstein Str., Rostok, 18059, Deutschland (Germany); ^bA. V. Luikov Heat and Mass Transfer Institute, National Academy of Sciences of Belarus, 15 P. Brovka Str., Minsk, 220072, Belarus; email: anchor@hmti.ac.by. Translated from *Inzhenerno-Fizicheskii Zhurnal*, Vol. 80, No. 2, pp. 46–59, March–April, 2007. Original article submitted July 15, 2005.

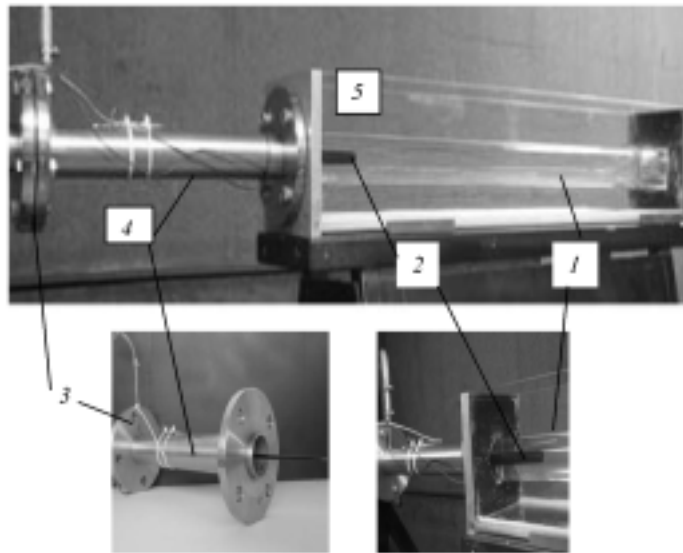


Fig. 1. Measuring portion of the channel: 1) external pipe of the mixer; 2) nozzle; 3) pluggable unit with a nozzle; 4) external pipe of unit 3; 5) box filled with water for diminishing optical distortion.

Investigations of the development of a scalar field for the mixing regimes noted above are few in number [3–7]. The regime of mixing without a recirculation zone in laminar flow of a medium out of the nozzle has been considered in [3], whereas the diagnostics of the scalar field in the regime of mixing with a recirculation zone with a 1-Hz frequency of sampling of instantaneous scalar distributions has been carried out in [4]. This circumstance made it possible to subsequently dispose of a comparatively small amount of information sufficient for calculating the first two statistical moments of turbulent characteristics. However, for the high moments and probability density functions of the scalar to be analyzed it must be at least doubled. More substantial is the fact that there are no simultaneous measurements of the velocity and scalar fields for the two mixing regimes indicated. This, undeniably, restricts the possibility of analyzing the interaction of such fields. The results obtained in the present experimental investigation make it possible to somewhat compensate for this drawback.

Apart from being of purely applied significance, the importance of experimental investigations is determined by the necessity of creating a database for testing modern theoretical mixing models using which one can calculate not only the averaged scalar field but also different statistical moments responsible primarily for the process of fine-structure mixing, i.e., micromixing. This process is characterized by the joint action of very small-scaled turbulent transfer and molecular diffusion. Information (obtained experimentally) on the distributions of the scalar and its pulsations opens up opportunities for checking the validity of the mathematical models used for the probability density functions of the scalar by comparing them to the probability functions calculated based on the measurements performed.

At the present time, one uses a few approximate analytical representations of the probability density function for scalar fields dependent on the statistical moments of the probability density function itself [8]. A two-parameter β distribution [9] which is widely used in different models of turbulent mixing and turbulent combustion of flows not mixed in advance is an example of such a function. In the work presented, we have compared such a β distribution to the analogous probability density function restored from the experimental distributions of the scalar and its pulsations.

Experimental Setup and Measurement Procedure. The experiment was performed in a closed-type water channel [5]. The mixer consisted of two coaxial pipes: pipe 1 ($D = 50$ mm) manufactured from Plexiglas and a steel nozzle 2 with an inside diameter of $d = 10$ mm (Fig. 1). The nozzle 2 was set up stationary in a pluggable unit 3 of length 430 mm. Pipe 4 had a movable joint to the flanges of the unit 3 via annular gaskets. Owing to this, the angular position of the nozzle relative to the pipe 1 was changed by rotation of the pipe 4. The axial alignment of the nozzle 2 over the length of pipe 4 was attained accurate to ± 0.3 mm. The assembly of the unit 3 ensured an axial alignment of pipes 1 and 4 no worse than ± 0.3 mm. The length of the nozzle's horizontal portion was equal to 550

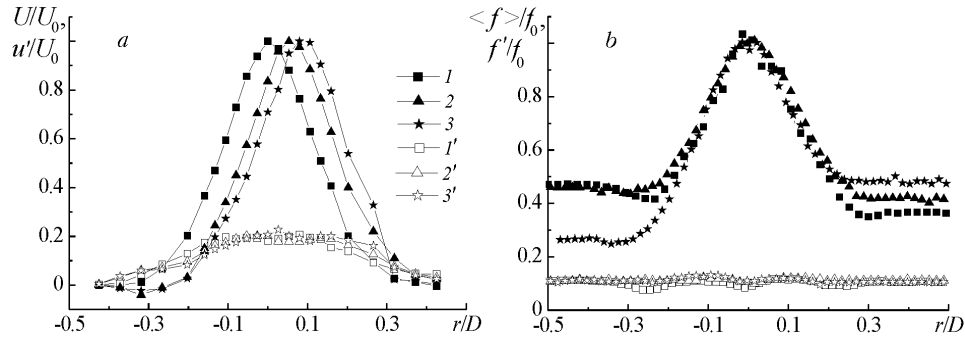


Fig. 2. Average values of the longitudinal velocity component U/U_0 (1–3) and its standard pulsations u'/U_0 (1'–3') (a) and the average values of the scalar $\langle f \rangle / f_0$ (1–3) and its standard pulsations f' / f_0 (1'–3') (b) in the cross section $x/D = 1.6$: 1 and 1') $\gamma = 0^\circ$, 2 and 2') 90° , and 3 and 3') 180° .

mm. The nozzle 2 extended 120 mm forward from the plane of the outlet cross section of the pipe 4. The lateral and lower walls of box 5 were manufactured from Plexiglas for optical diagnostics of flow in the mixer. Filling the box 5 with water diminished the optical distortion caused by different degrees of refraction of a laser beam in air, Plexiglas, and water and by the curvature of the pipe 1.

The velocity was measured with a Dantek one-component Doppler laser anemometer (Flow Light 1). The profiles of the average velocity and velocity pulsations were recorded in the mixer cross sections beginning with a distance of 1 mm from the nozzle outlet section to 9 calibers (of the mixer diameter) downstream for three angular positions of the nozzle (0° , 90° , and 180°); the position presented in Fig. 1 was considered as the first one (0°).

The concentration of the passive impurity was measured by the LIF (Laser Induced Fluorescence) method. An aqueous solution of 6G rhodamine with a concentration of 0.03 mg/liter, flowing out of the nozzle, was used as the fluorescent substance. The measuring system incorporated a pulsed Nd:YAG laser emitting light of wavelength 532 nm with a pulse duration of 7 nsec, a CCD camera (PI-MAX, Roper Sci. Corp), and optical lenses [4]. The laser knife was formed by the lenses in the vertical plane coincident with the axis of the mixer and the flow. The camera recorded the instantaneous intensity of radiation of the mixture in the laser-knife plane one pixel wide along the mixer's diameter; the information obtained was transmitted to a computer. Unlike the investigations performed earlier [4, 5], the rate of data transmission was limited just by the frequency (10 Hz) of the laser used as the external trigger of the camera. For each mixer cross section diagnosed, we recorded a file containing 1000 instantaneous intensity distributions. The measurement time was 100 sec. A threefold increase in the recording time exerted virtually no influence on the values of the average and pulsation characteristics of the scalar and led to a 5% change in the values of the probability density function. Setting up an intermediate ring (Nikon PK-11A) between the camera and the objective (Nikorr 50 mm) made it possible to increase the spatial resolution to 0.3 mm. The position of the camera relative to the laser knife remained constant with its movement along the mixer axis. The velocity and the intensity of radiation were measured in the same cross sections of the mixer.

The scalar field in the cross section of the mixer was characterized by a distribution of the mixture coefficient f equal to the ratio of the local intensity of radiation of the fluorescent substance to its maximum intensity on the jet axis in the cross section $x/D = 0.1$. The degeneration of the scalar along the mixer axis was evaluated by the change in the mixture coefficient in normalizing its running value to the value measured on the axis in the cross section $x/D = 0.1$.

The development of the velocity and scalar fields was investigated for the flow-rate ratios Q_D/Q_d ensuring the regimes of mixing with a recirculation zone ($Q = Q_D/Q_d = 1.3$) and without it ($Q = 5.0$). The flow of the jet out of the nozzle for $Re_d = 10,000$ was turbulent in all cases.

Investigation Results. Due to the reflection of the laser beam from the mixer walls, the signal of the Doppler laser anemometer at a distance of ~ 4 mm from the walls was unstable and the diagnostics of the velocity and velocity pulsations was impossible in this flow region.

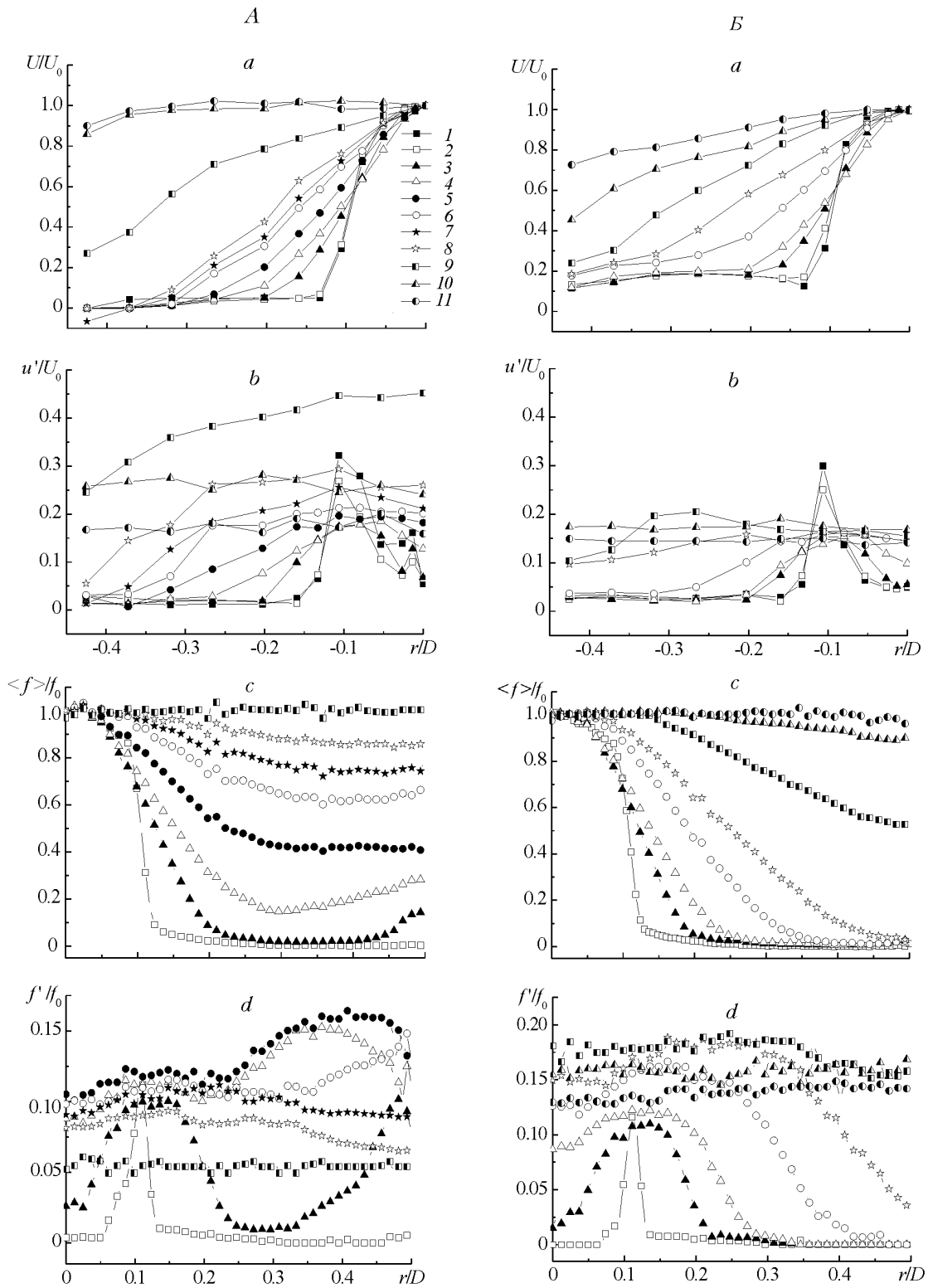


Fig. 3. Distributions of the average values of the longitudinal velocity component U/U_0 (a) and its standard pulsations u'/U_0 (b) and the average values of the scalar $\langle f \rangle / f_0$ (c) and its standard pulsations f' / f_0 (d) over the mixer cross section at different distances from the nozzle: A) $Q = 1.3$, B) $Q = 5$ [1] $x/D = 0; 2) 0.1; 3) 0.6; 4) 1.1; 5) 1.6; 6) 2.1; 7) 2.6; 8) 3.1; 9) 5.1; 10) 7.1; 11) 9.1$].

The velocity and scalar profiles in the regime of mixing with a recirculation zone that have been measured for three angular coordinates of the unit 3 (Fig. 1) point to the flow asymmetry in the mixer (Fig. 2). A possible reason for this asymmetry is the mismatch of the nozzle axis and the mixer axis because of the fact that the pipes 1 and 4 used in the mixer's structure had a certain ellipsoidal shape inherent in regular commercial pipes. Such a deviation from a cylindrical shape could result in a maximum mismatch (to 1 mm) of the nozzle axis and the mixer axis.

Because of the dissimilar degrees of distortion of flow in different planes, we selected a plane in which the flow symmetry was the highest for comparative analysis of the development of hydrodynamic and scalar parameters. Since the velocity and the scalar were measured in mutually orthogonal planes, we compared the velocity distribution in the 0° plane and the corresponding scalar distributions in the 90° plane (Fig. 3).

Backflow is realized in a thin layer near the wall and is recorded by the change of sign of the average velocity just in the cross section $x/D = 2.6$ (Fig. 3Aa). Thus, it seems impossible to establish the boundaries of the recirculation zone from the average-velocity profiles. Nonetheless, their change for $x/D > 3.1$ points to the apparent rearrangement of the flow structure. In [2], backflow was observed in the range of distances from the nozzle $0.4 \leq x/D \leq 3.0$ for an analogous mixing regime but with somewhat different parameters $Q = 1.02$ and $D/d = 13.5$. Barchilon and Curtet [2] also established that increase in the parameter Q was accompanied by the downstream shift of the leading edge and center of the recirculation zone, whereas the boundary of its degeneration remained constant for $x/D \approx 3.0$.

In the present investigation, the level of turbulent pulsations grew over the mixer cross section downstream from the nozzle, reflecting the development of the recirculation zone, which is consistent with the pulsation dynamics described in [2]. However the maximum turbulent velocity pulsations were recorded immediately behind the recirculation zone in the cross section $x/D = 5.1$, not in this zone. The formation of a uniform velocity distribution over the mixer cross section ($x/D < 5.1$) became responsible for the decrease in the pulsations (Fig. 3Ab).

The scalar distributions point to the fact that backflow occurs beginning with the distance $x/D \geq 0.6$ and the concentration of the passive impurity at the mixer walls grows (Fig. 3Ac). The average-scalar profile becomes wider downstream more rapidly than the average-velocity profile. As a result, we observe macromixing, i.e., the formation of a quasihomogeneous composition of the mixture over the mixer cross section, at the distance $x/D = 5.1$ now, which is much earlier than the formation of the uniform average-velocity distribution ($x/D > 9.1$).

An analysis of the development of the profiles of the average scalar and its pulsations makes it possible to refine the coordinates of the boundaries of the recirculation zone. Clearly, scalar pulsations must grow at the boundary of interaction of the backflow with the flow in the pipe 1. The high level of scalar pulsations in the wall region ($r/D > 0.4$ and $x/D = 0.6$) extends downstream to the coordinate $r/D > 0.3$ ($1.1 \leq x/D \leq 1.6$), after which it begins to diminish. From the physical representations, it is clear that the scalar distribution is close to a locally homogeneous state. On the basis of these representations, it may be stated that the recirculation zone begins behind the cross section $x/D = 0.1$ and degenerates to the cross section $x/D < 5.1$; its center is in the interval $2.1 < x/D < 2.6$ (Fig. 3Ac, d) and d). Thus, the recirculation-zone length in this case is larger than that established in [2]. This fact is determined by the geometry of the mixers in question, namely, by the difference in the D/d ratio [6].

The regime of mixing without a recirculation zone is characterized by a higher velocity of the cocurrent flow and a monotonic expansion of the velocity profile reflecting the development of jet flow (Fig. 3B). When $x/D < 2.1$ the profiles of turbulent pulsations are much narrower, and their maximum values are lower than those in the mixing regime considered above. Despite the fact that the average-velocity distribution over the mixer cross section is far from being uniform in the range of distances $x/D < 9.1$ studied, the turbulent-pulsation profiles in the cross sections $x/D = 7.1$ and 9.1 are quite uniform. Their values are noticeably lower than those existing in analogous cross sections in the regime of mixing with a recirculation zone where the average-velocity distribution is more uniform. Mixing without a recirculation zone is slower, and a quasiuniform scalar distribution begins to be realized only when $x/D = 9.1$. The change in the scalar field is, undeniably, a result of the development of a hydrodynamic field; nonetheless, the average-scalar field becomes wider appreciably more rapidly than the average-velocity profile. Since the Schmidt number is large ($Sc > 1000$) for the media in question, i.e., diffusive scalar transfer is insignificant compared to convective transfer, the more rapid expansion of the average-scalar profile may be caused just by the high level of intermittence at the jet boundary. The intermittence is related to the nonstationary vortices in the shearing layer, whose size grows downstream. The average-velocity profiles reflect just the most probable position of the boundary of jet flow, ignoring,

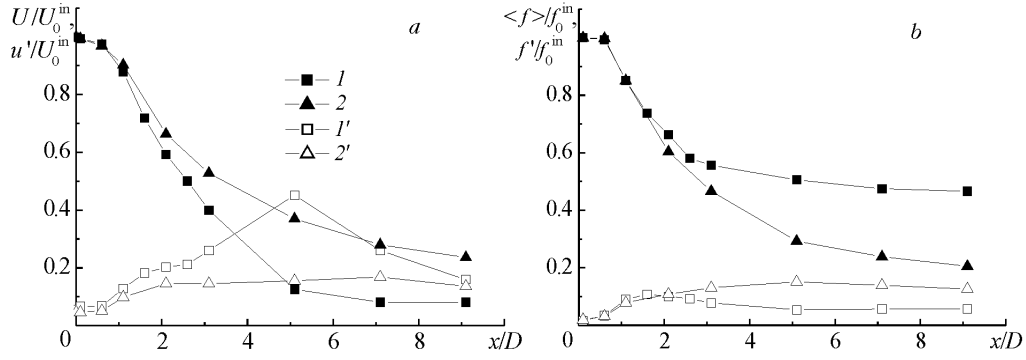


Fig. 4. Degeneration of the average value of the longitudinal velocity component U/U_0^{in} (1, 2) and its standard pulsations u'/U_0^{in} (1', 2') (a) and of the average scalar $\langle f \rangle / f_0^{\text{in}}$ (1, 2) and its standard pulsations f'/f_0^{in} (1', 2') (b) along the mixer axis in different mixing regimes: 1 and 1') $Q = 1.3$ and 2 and 2') $Q = 5$.

in fact, the nonstationary character of this boundary, which manifests itself in the average-scalar distributions. The profiles of standard scalar pulsations also turned out to be more sensitive to the nonstationary character of flow. They are wider near their maximum values compared to the profiles of velocity pulsations and expand appreciably more rapidly than the latter. The values of scalar pulsations in the region where macromixing is attained are close to the level of velocity pulsations. In the mixer cross section $x/D = 9.1$, they are nearly threefold higher than the values obtained in the regime of mixing with a recirculation zone.

The character of degeneration of the average values of the velocity and the scalar along the mixer axis demonstrate that, up to the distance $x/D = 1.6$, the dynamics of degeneration of the average scalar is determined solely by the degeneration of the average jet velocity (Fig. 4). The influence of the nonstationary behavior of vortices at the jet boundary on the scalar transfer is still insignificant by virtue of the small scale of these vortices.

Such a situation holds for the regime of mixing without a recirculation zone with a certain leading rate of degeneration of the average scalar downstream, whereas scalar pulsations change virtually as velocity pulsations. In the regime of mixing with a recirculation zone, the average velocity on the mixer axis immediately behind the cross section $x/D = 1.6$ degenerates more rapidly, and the degeneration of the average scalar, conversely, slows down. Velocity pulsations grow from the nozzle outlet section downstream, attain their maximum in the cross section $x/D = 5.1$, and rapidly degenerate to the cross section $x/D = 9.1$ in which approach values determined in the regime of mixing without a recirculation zone. Scalar pulsations also grow downstream but only to the distance $x/D \approx 2$. Next they decrease and, beginning with the cross section $x/D = 5.1$, virtually do not change, remaining, as has already been noted, nearly threefold lower than the values of pulsations in the regime of mixing without a recirculation zone. This demonstrates that a higher degree of mixing in the quasihomogeneous state is attained when a recirculation zone is formed in the mixer.

Additional information on the development of flow for both mixing regimes may be obtained by analysis of the values of an autocorrelation function calculated from the instantaneous scalar distributions $f(y)$:

$$R_f(r, \eta) = \frac{\langle f'(r)f'(r+\eta) \rangle}{\sqrt{\langle f'^2(r) \rangle} \sqrt{\langle f'^2(r+\eta) \rangle}}. \quad (1)$$

In Fig. 5, the autocorrelation function (1) is constructed at different distances from the nozzle for three points of the mixer cross sections. This enables one to track the behavior of flow at each analyzed point. The autocorrelation function with a narrow peak of unity points to the flow regions where the values of the average scalar are nearly constant. Clearly, scalar pulsations are minimum in these regions, which determines the zero value of the function at a small distance from the coordinate analyzed. This fact is observed at each point of the flow in the initial cross section of the mixer $x/D = 0.1$.

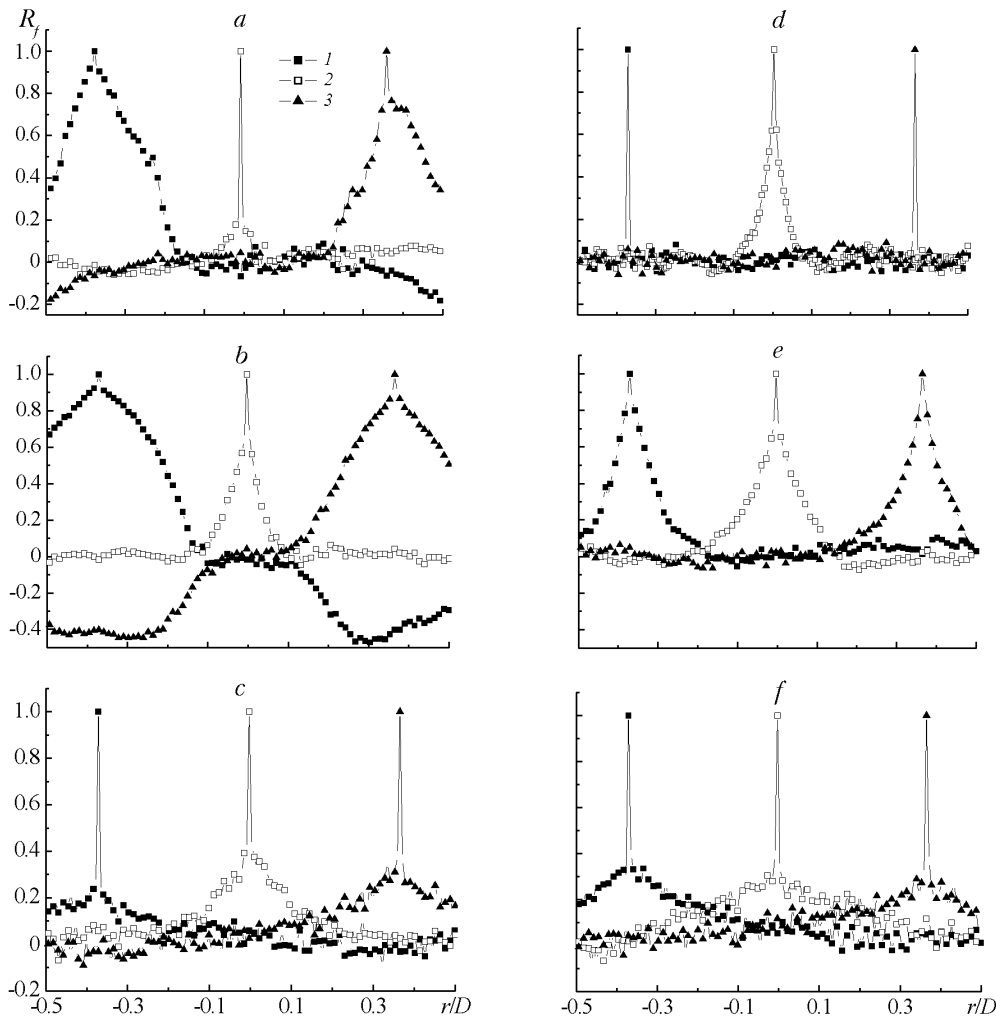


Fig. 5. Distributions of the autocorrelation function for three points of the mixer cross section r/D [1] $r/D = -0.37$, 2) 0, and 3) 0.37] in two mixing regimes [a–c] $Q = 1.3$ and d–f) $Q = 5$ at different distances from the nozzle: a) $x/D = 0.6$; b) 1.6; c and e) 3.1; d) 1.1; f) 9.1.

For the regime of mixing with a recirculation zone, the situation substantially changes even in the cross section $x/D = 0.6$. Regions of strong correlation are formed in the mixer near the walls (Fig. 5a). For each point for $r/D = -0.37$ and 0.37 the correlation approaches zero in the direction of the jet and, changing sign to negative, grows in value again near the opposite wall. The change of correlation sign is a result of the phase shift of pulsations by 180° at the points in question according to (1). The negative correlation points to the existence of flow in the opposite direction near the mixer walls. Indeed, such a vibrational motion of the medium in the wall region is observed in visualizing the flow, which is consistent with the instantaneous pattern of visualization performed in [2]. The correlation regions near the walls decrease in size downstream (Fig. 5b and c) and completely degenerate for $x/D = 5.1$, which is characteristic of a quasihomogeneous mixture. On the jet axis, the profile of the autocorrelation function monotonically expands downstream due to the decrease in the concentration of the passive impurity (Fig. 5a–c). It is characteristic that the flow structures on the mixer axis virtually do not correlate with the structures in the recirculation zone. Clearly, this is a consequence of the small scale of such structures. For the region of a quasihomogeneous mixture for $x/D \geq 5.1$, the autocorrelation function represents the distribution with a narrow peak of unity again.

In the regime of mixing without a recirculation zone, the change in the profile of the autocorrelation function for the points $r/D = -0.37$ and 0.37 demonstrates that, in the regions in question, we have no mixing of the cocurrent

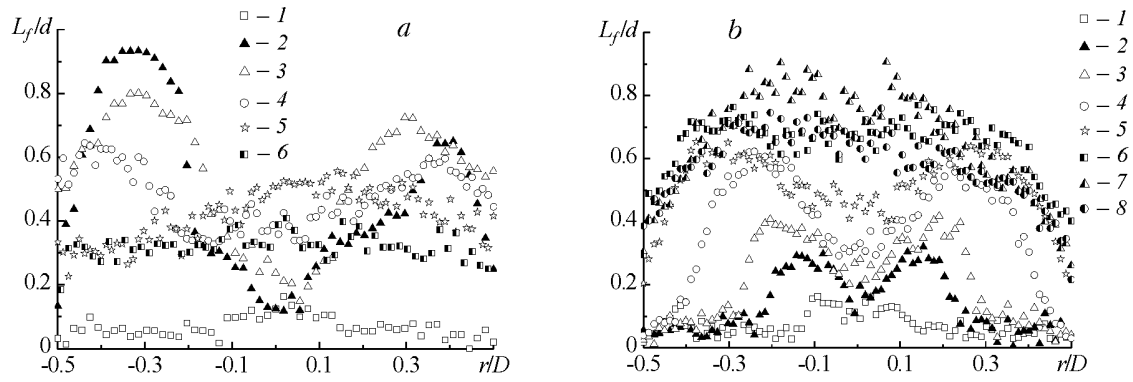


Fig. 6. Change in the integral scale in the mixer cross section at different distances from the nozzle: a) $Q = 1.3$ [1] $x/D = 0.1$; 2) 0.6; 3) 1.1; 4) 2.1; 5) 3.1; 6) 5.1]; b) $Q = 5$ [1] $x/D = 0.1$; 2) 0.6; 3) 1.1; 4) 2.1; 5) 3.1; 6) 5.1; 7) 7.1; 8) 9.1].

flow with the jet up to the distances $x/D > 2.1$ (Fig. 5d). As the jet diverges, its vortex structures fill the entire volume in the mixer, which is reflected in the appearance of a correlation near the mixer walls for $x/D = 3.1$. At the distance $x/D = 9.1$, the distribution of the autocorrelation function is analogous to its distribution observed for the regime of mixing with a recirculation zone in the cross section $x/D = 3.1$. Thus, it may be inferred that macromixing has yet to be attained and will be completed downstream.

The integral scale in the mixer cross section is calculated using the autocorrelation function R_f :

$$L_f(r) = \int_{-\infty}^{\infty} R_f(r, \eta) d\eta. \quad (2)$$

This dependence rigorously holds for the quasihomogeneous state of the mixture; therefore, when there are different scales in the flow region analyzed, the information obtained on the change in the integral scale is qualitative in character (Fig. 6). The integral-scale distributions are made dimensionless by means of the nozzle diameter d . In the initial cross section of the mixer $x/D = 0.1$, the values of the integral scale are small and its distribution is quite uniform.

The maximum values of the integral scale for the mixing regimes in question are virtually identical but are realized at different distances from the nozzle and from the mixer axis. In the regime of mixing with a recirculation zone, the maximum L_f values are attained in the region between the jet boundary and the mixer wall in the cross section $x/D = 0.6$ (Fig. 6a). They monotonically decrease downstream, whereas the integral scale on the jet axis grows. In the cross section $x/D = 3.1$, the values of L_f on the mixer axis are nearly twice as high as the values of this quantity in the wall region. Such a change in the parameter L_f reflects, first (as has already been noted in analyzing the behavior of the autocorrelation function), the independent character of development of the jet and the recirculation zone and, second, the size reduction of the structures of this zone in its degeneration. Thus, the transfer scales in the recirculation zone significantly differ along its length and it is incorrect to represent this zone as a stationary vortex formation without allowance for its nonstationary behavior. In the region of macromixing, the values of the integral length scale are minimum and its distribution over the mixer cross section is quite uniform.

In the regime of mixing without a recirculation zone (Fig. 6b), the change in the integral scale corresponds to the development of the jet: the maximum L_f values are observed in the shearing layer and increase with its expansion. The external jet boundary joins the mixer walls at the distance $x/D = 3.1$. Beginning with the cross section $x/D = 5.1$ the integral scale remains constant in the wall region but it grows on the mixer axis, attaining its maximum values in the cross section $x/D = 7.1$. The formation of a uniform integral-scale distribution just in the region near the mixer axis at a distance of 9 calibers from the nozzle confirms the conclusion that macromixing in the range of distances x/D investigated is incomplete.

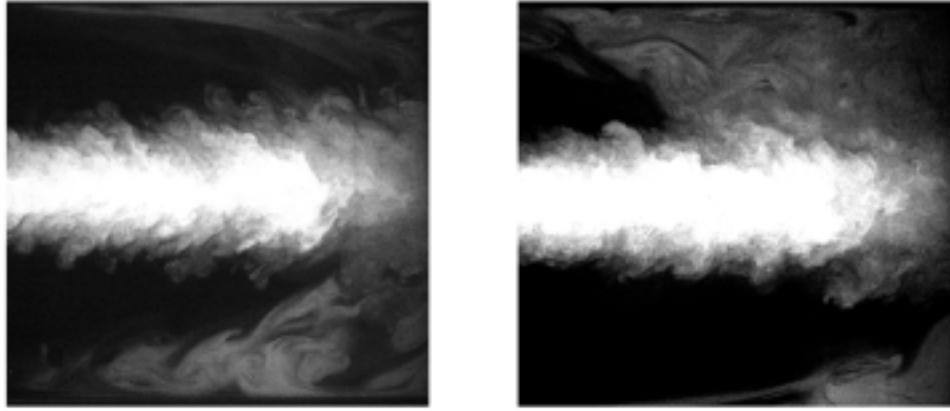


Fig. 7. Photographs of the instantaneous scalar field in the mixing regime with a recirculation zone taken with an interval of 1 sec.

It is characteristic that the development of the integral scale on the jet axis to the cross section $x/D = 3.1$ in both mixing regimes considered is similar. The change in this parameter downstream is significantly different: it decreases in the regime of mixing with a recirculation zone and grows in the regime of mixing without a recirculation zone. Clearly, the increase in this scale is determined by the continuing growth in the jet's vortex structures, whereas its decrease is a consequence of the destruction of the recirculation zone; this destruction also leads to a degeneration of vortex structures on the mixer axis due to the intense interaction of the vortex structures of the recirculation zone and the jet. The increase in the level of turbulent pulsations on the mixer axis (Figs. 3Aa and 4a) is, apparently, a reflection of the process observed.

The above analysis of the parameters of the velocity and scalar fields has revealed new features of the formation of a recirculation zone that manifest themselves to full measure in flow visualization (Fig. 7). First of all, this means the existence of a narrow backflow layer along the mixer walls, nearly reaching the nozzle exit section. Video recording of the process of mixing during 17 sec has shown that flow in the recirculation zone vibrated near the walls in opposition with a period of ~ 5 sec. The negative correlation between the points of this zone at the opposite mixer walls (Fig. 5b) reflects the process observed. The instantaneous picture of the recirculation zone, representing a superposition of numerous nonstationary vortices of different scale (Fig. 7), is in satisfactory agreement with the results of the analysis of the integral-scale distributions (Fig. 6).

The first stage of formation of a homogeneous state of the mixture is in attaining macromixing, i.e., equalization of the values of the average scalar over the mixer cross section occurs. This process is completed in the regime of mixing with a recirculation zone and has to be completed in the regime without a recirculation zone. The complete mixing of the mixture, however, is characterized by the termination of the process of mixing when the values of scalar pulsations degenerate throughout the mixer cross section [8]. The state of the process of micromixing may be judged from the form of the scalar's single-point probability density function, which is a good criterion of fine-structure mixing related to the interaction of very small-scaled turbulent transfer and molecular diffusion in the flow [9]. Unlike the statistical moments (average value, standard scalar pulsations, and other moments) describing the integral properties of the scalar field, such a function contains probabilistic information on all scalar values that may be present at a given point of the flow.

The probability density function in the mixture mixed to molecular scales is characterized by the δ function, whereas the quasihomogeneous state of the mixture is described by the Gaussian distribution. The probability density function is determined with the use of experimental instantaneous scalar distributions as

$$P_{\text{exp}}(f) = \lim_{N \rightarrow \infty} \frac{N_h(f)}{Nh} . \quad (3)$$

We compare the function (3) obtained experimentally to the probability density function theoretically calculated in the form of a β distribution [10]:

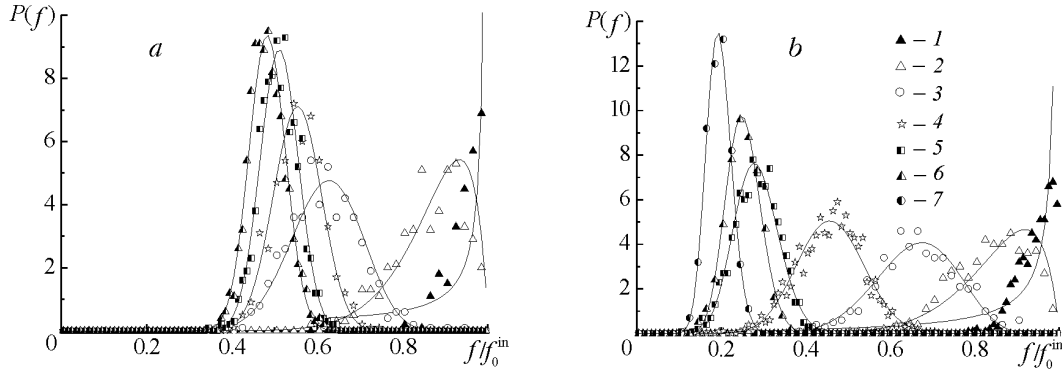


Fig. 8. Experimental probability density function of the scalar (3) compared to the theoretical probability density function in the form of β distribution (4) (curves) on the mixer axis at different distances from the nozzle: a) $Q = 1.3$ and b) $Q = 5$ [1] $x/D = 0.6$; 2) 1.1; 3) 2.1; 4) 3.1; 5) 5.1; 6) 7.1; 7) 9.1].

$$P(f) = \frac{f^{\alpha-1} (1-f)^{\beta-1}}{\int_0^1 f^{\alpha-1} (1-f)^{\beta-1} df}. \quad (4)$$

Two positive parameters α and β in (4) are dependent [10] on the average value of the scalar $\langle f \rangle = \int_0^1 fP(f)df$ and the

variance of the scalar $f'^2 = \int_0^1 (f - \langle f \rangle)^2 P(f)df$:

$$\alpha = \langle f \rangle \left[\frac{\langle f \rangle (1 - \langle f \rangle)}{f'^2} - 1 \right], \quad \beta = \alpha \frac{1 - \langle f \rangle}{\langle f \rangle}.$$

The statistical moments of higher order — asymmetry Sk and excess Ku — are related to the intermittence determined by the existence of a wide range of length scales in the flow. These moments determined from the experimental scalar distributions as

$$Sk = \frac{1}{N} \sum_{n=1}^N \left(\frac{f_n - \langle f \rangle}{f'} \right)^3, \quad Ku = \frac{1}{N} \sum_{n=1}^N \left(\frac{f_n - \langle f \rangle}{f'} \right)^4, \quad (5)$$

may be used for obtaining data on the profile of the probability density function.

The asymmetry Sk characterizes the degree of mixing of the profile of the probability density function relative to the average value of the scalar $\langle f \rangle$, and the excess Ku points to the degree of flatness of this function compared to its Gaussian form $P_G(f) = \frac{1}{\sqrt{2\pi}f'^2} \exp \left\{ -\frac{(f - \langle f \rangle)^2}{2f'^2} \right\}$, which is responsible for the asymptotic quasihomogeneous state of the medium. The Gaussian distribution is symmetric; therefore, we have $Sk = 0$ and $Ku = 3$.

Change in the probability density function for both mixing regimes along the mixer axis shows their difference even at the distance $x/D > 0.6$ (Fig. 8).

The inconsistency between the probability density functions calculated from relations (3) and (4) is maximum in the initial cross sections of the mixer and decreases downstream. Thus, the use of the β distribution for modeling

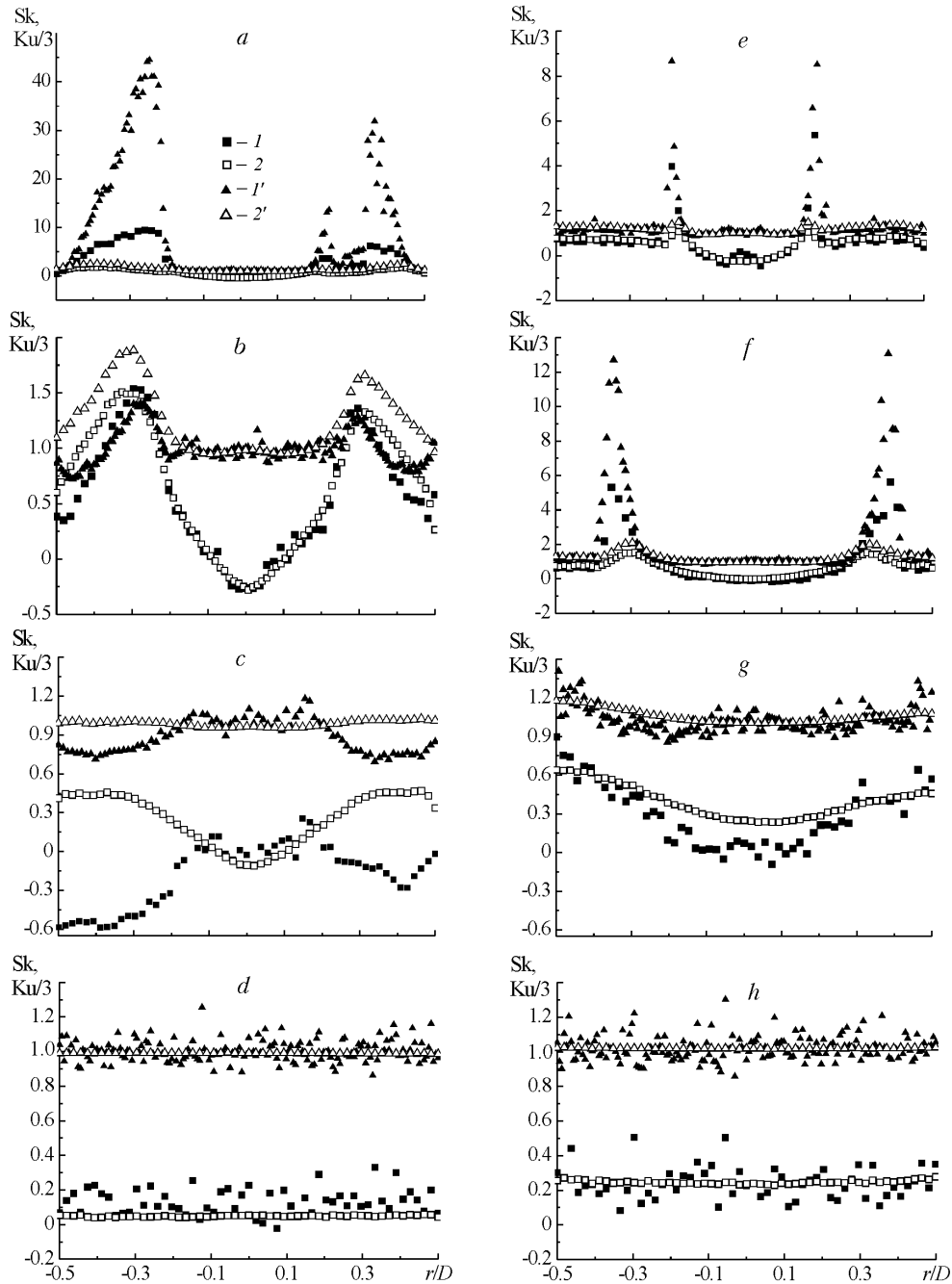


Fig. 9. Distributions of the asymmetry (1, 2) and excess (1', 2') coefficients over the mixer cross section for two mixing regimes [a-d] $Q = 1.3$; e-h] $Q = 5$] at different distances from the nozzle: a and e) $x/D = 0.6$; b) 1.1; c) 1.6; d and g) 5.1; f) 2.1; h) 9.1 (1 and 1', Sk and $Ku/3$ values obtained experimentally; 2 and 2') the same parameters calculated from the theoretical probability density function in the form of β distribution (4)).

mixing on the initial jet portion is quite arbitrary. This theoretical model well describes experimental probability density functions for the mixture approaching a quasihomogeneous state ($x/D > 2.1$ for $Q = 1.3$ and $x/D > 7.1$ when $Q = 5$). The final form of the probability density function is far from that of the δ function, which confirms the conclusion on the incompleteness of the micromixing for the two regimes considered.

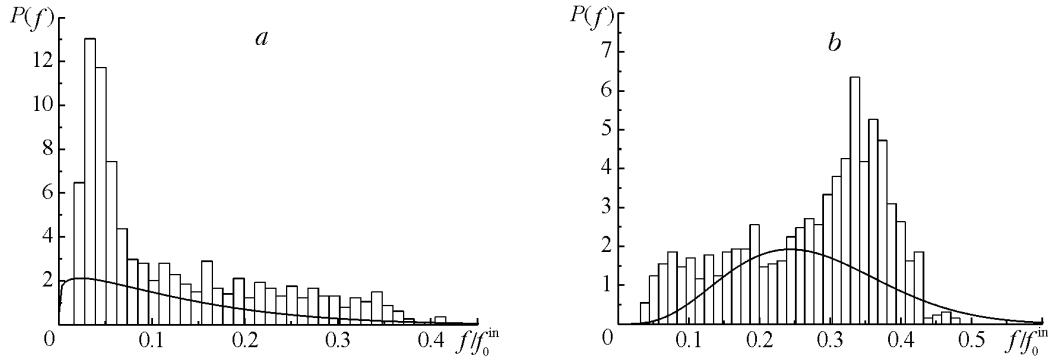


Fig. 10. Probability density function of the scalar for the point of the recirculation zone with coordinates $r/D = -0.37$ in the cross sections $x/D = 1.1$ (a) and $x/D = 1.6$ (b) (curves, theoretical probability density function in the form of β distribution (4), columns, experimental probability density function).

An analysis of the change in the probability density function in the mixer cross section is performed with the use of the asymmetry Sk and excess Ku coefficients. These statistical moments are compared using the probability density function determined experimentally and β distribution (4) (Fig. 9).

Two strong-intermittence regions characterized by the high values of high moments are developed immediately behind the nozzle in the regime of mixing with a recirculation zone. The positive maximum of the asymmetry Sk reflects the fact that the probability of low values of the scalar is very high, i.e., the profile of the probability density function is extended toward higher scalar values, which is characteristic of the wall region of flow. The negative asymmetry on the jet axis is caused by the cocurrent flow being involved in the jet and by the reduction in the concentration of the initially homogeneous passive impurity in it. In the cross section $x/D = 0.6$, the intermittence is strong near the mixer wall, whereas at the jet boundary, it shows itself only slightly (Fig. 9a). The intermittence rapidly degenerates downstream, but the regions with different asymmetry signs are preserved to the distance $x/D = 1.6$.

In the region of strongest intermittence, the asymmetry Sk and the excess Ku characteristic of the β distribution do not reflect the change in analogous statistical moments calculated from experimental data; however a qualitative agreement between them is observed in the cross section $x/D = 1.1$.

At the distance $x/D = 1.6$, the experimental asymmetry profile is mirror-type relative to the profile determined from the probability density function in the form of β distribution (4). The values of the excess Ku point to the substantial deviation of the experimental probability density function from the Gaussian distribution, unlike the values calculated from the theoretical probability density function. We emphasize that the drawback of the a priori approach to specifying the form of the probability density function (this form is determined just by the first two statistical moments of the scalar field — the average value of the scalar and its standard pulsation) is the most pronounced in the distributions of the parameters Sk and Ku in the cross section $x/D = 1.6$. Indeed, the data presented and the results of a number of investigations show that the statistical properties of the flow at different points of the mixer may be described by a more complex (e.g., bimodal) form of the probability density function, whose two-parameter representation becomes not sufficiently faithful [8, 9] (Fig. 10). In this case it is necessary to use a larger number of statistical moments for restoration of the probability density function, which follows from the theorem of probability theory according to which information contained in the set of moments of all orders and in the distribution function is equivalent. One method developed within the framework of statistical physics is the method of restoration of the probability density function; it is based on the hypothesis that the computed form of this function must ensure the statistical-entropy maximum and be compatible with information on the existing moments of the corresponding random fields [11].

Upon the completion of macromixing ($x/D = 5.1$), the values of the excess Ku of the probability density under study are consistent with the value characteristic of the Gaussian distribution, but the values of the asymmetry Sk are nonzero. However, Sk values found from β distribution (4) are lower than the corresponding values characterizing the probability density functions constructed on the basis of experimental data (Fig. 9d).

The use of the β distribution as the model for the probability density function adequately describing the actual processes of mixing for the regime of mixing without a recirculation zone is beyond question (Fig. 9e–h). Certain problems of agreement of the change in the model probability density function (4) with the experimental probability density function are preserved in the narrow zone of intermittence at the jet boundary. The possibility of using the β distribution for description of the scalar distribution on the mixer axis has been noted in [3].

Conclusions. The experimental investigations performed for two regimes of mixing in an axisymmetric jet mixer have shown a significant difference in the dynamics of formation of a velocity field. In the range of distances $0.1 \leq x/D \leq 9.1$ investigated, a uniform distribution of the average velocity has no time to be formed, although, in formation of a recirculation zone, a uniform velocity distribution is established along most of the mixer cross section. The profiles of turbulent pulsations in both mixing regimes are quite homogeneous beginning with the distance $x/D \geq 7.1$, and their values for the corresponding cross sections are higher in the regime of mixing without a recirculation zone.

In the regime of mixing with a recirculation zone, the formation of a quasihomogeneous scalar field, or the completion of macromixing, is carried out to the cross section $x/D = 5.1$. In the regime of mixing without a recirculation zone, this process only nears completion in the cross section $x/D = 9.1$. In the first case, the level of scalar pulsations in the quasihomogeneous state is nearly threefold lower than that in the second.

Thus, the development of the scalar field leads the development of the velocity field. Since scalar transfer is determined by the flow dynamics (in this work, we have $Sc > 1000$), the more rapid development of the scalar field is attributable to the influence, on the transfer, of nonstationary vortices generated in the mixing layer and ensuring scalar transfer to a larger distance than the jet boundary determined statistically. The averaging of the dynamic characteristics of the flow conceals the influence of such vortices; however the scalar field formed by them points to their decisive role in the process of mixing. Consequently, consideration of the development of the velocity field as a stationary process even in the case of the regime of mixing without a recirculation zone does not reflect the actual physical phenomenon. Therefore, the use of statistical turbulence models based on the averaged characteristics of the velocity field for calculations of the scalar field leads to erroneous conclusions. Such calculations must, apparently, be performed with more perfect approaches, e.g., the LES (Large Eddy Simultaneous) method.

In mixing to form a backflow zone, neglect of the nonstationary behavior of a recirculation zone totally misinterprets its physical nature. Visualization of the recirculation zone and an analysis of the change in the autocorrelation function clearly demonstrate the nonstationary character of this flow. Vibrational motion near the walls of the mixer in opposition for regions symmetric about its axis manifests itself in the change of sign of the autocorrelation function constructed from the scalar distribution. Also, this function demonstrates the absence of the interaction between the structures of the recirculation-zone and the jet core, which is a consequence of their small size. The structure of this zone represents a superposition of nonstationary vortices of different size, not one stationary vortex with a length to three calibers.

An analysis of the change in the probability density function and the asymmetry and excess distributions shows how far the running state of the mixture from the complete mixing or a homogeneous state is and the manner in which macromixing transforms to micromixing. For the two regimes considered, micromixing is not completed in the investigated range of distances. An analysis of the applicability of the probability density function in the form of a β distribution to calculation of the scalar field demonstrates its untenability for the region of strong intermittence, where we have not only a great deal of discrepancy between the calculated and experimental values of the asymmetry and excess but also observe their qualitatively different behavior.

The reason why the asymmetry of flow of the recirculation zone occurs is not quite clear. The previous investigations [4, 5] in which this asymmetry was found for the first time were characterized by more significant errors in the mixer structure, but their elimination is seen to fail to ensure the desired symmetry of flow. It is highly probable that the flow asymmetry near the nozzle is caused by the jet itself. This is confirmed by the observed process of interaction between the jet and the recirculation zone, which causes the jet to deflect [2]. The calculations of this flow type that are being completed at present by the LES method enable one to establish the possibility of the asymmetry being formed in an axisymmetric jet mixer.

The work was carried out with support from the German Foundation for Basic Research (SPPP 1141) and the Belarusian Republic Foundation for Basic Research (T06MC-042).

NOTATION

D , inside diameter of the mixer; d , inside diameter of the nozzle; f , coefficient of the mixture (scalar); $\langle f \rangle$, average value of the scalar; f' , standard scalar pulsation; f_n , value of the scalar in the n th measurement; f_0 , values of the average scalar on the mixer axis; h , step of subdivision of the definition domain of the scalar $f \in [0, 1]$; K_u , excess of the scalar; L_f , integral length scale; N , number of measurements; $N_h(f)$, number of realizations with the scalar value fallen within the band $[f-h, f]$; $P(f)$, probability density function of the scalar; Q , ratio of the volume flow rates at exit from the nozzle and of the cocurrent flow; Q_D , volume flow rate of the cocurrent flow; Q_d , volume flow rate of the jet at exit from the nozzle; Re_d , Reynolds number calculated from the nozzle parameters; R_f , autocorrelation function; Sc , Schmidt number; Sk , asymmetry of the scalar; U , average value of the longitudinal velocity component; U_0 , average value of the longitudinal velocity component on the mixer axis; u' , standard pulsation of the longitudinal velocity component; x and r , coordinates along and across the mixer; α and β , parameters of the β distribution; γ , angular coordinate of unit 3 (Fig. 1); η , shear in the autocorrelation function; δ , Dirac function. Subscripts and superscripts: exp, quantity determined experimentally; in, value in the mixer cross section near the nozzle outlet; n , measurement No.

REFERENCES

1. H. J. Henzler, Investigations on mixing fluids, Doctoral Dissertation, RWTH, Aachen (1978).
2. M. Barchilon and R. Curtet, Some details of the structure of an axisymmetric confined jet with backflow, *J. Basic Eng.*, No. 12, 777–787 (1964).
3. M. Mortensen, W. Orciuch, M. Bouaifi, and B. Andersson, Mixing of a jet in a pipe, *Chem. Eng. Res. Design*, **82**, No. 3, 357–363 (2004).
4. V. L. Zhdanov, N. V. Kornev, and E. Hassel, LIF investigation of the concentration field in the co-axial mixer, *Lasermethoden in der Strömungsmesstechnik*, 12 Fachtagung, 7–9 September 2004, Karlsruhe: Universität Karlsruhe (2004), pp. 16-1–16-8.
5. V. L. Zhdanov, A. D. Chorny, N. V. Kornev, and E. Hassel, Formation of the field of concentration of a passive impurity in an axisymmetric mixer, *Dokl. Nats. Akad. Nauk Belarusi*, No. 4, 115–119 (2005).
6. V. L. Zhdanov, N. V. Kornev, and E. Hassel, The influence of the mixer geometry on the scalar field formation, *Lasermethoden in der Strömungsmesstechnik*, 13 Fachtagung, 6–8 September 2005, Cottbus, Germany (2005), pp. 37-1–37-8.
7. V. L. Zhdanov, A. D. Chorny, N. V. Kornev, and E. Hassel, Formation of a homogeneous scalar field in an axisymmetric mixer, in: *Proc. 4th Int. Conf. on Heat Transfer, Fluid Mechanics and Thermodynamics* (HEFAT-2005), 19–22 September 2005, Cairo (2005), Paper ZV2.
8. P. A. Libby and F. H. Williams (Eds.), *Turbulent Reacting Flows*, Academic Press, London–New York (1994).
9. V. A. Sosinovich, *On the Theoretical Description of Turbulent Mixing of Scalar Fields*, Preprint No. 20 of the A. V. Luikov Heat and Mass Transfer Institute, National Academy of Sciences of Belarus, Minsk (1986).
10. R. P. Rhodes, A probability distribution function for turbulent flows, in: S. N. B. Murthy (Ed.), *Turbulent Mixing in Nonreactive and Reactive Flows*, Plenum Press, New York (1975), pp. 235–241.
11. S. B. Pope, A rational method of determining probability distributions in turbulent reacting flows, *J. Non-Equil. Thermodyn.*, **4**, 309–320 (1979).